Molecular Docking and 3D-QSAR Studies on Gag Peptide Analogue Inhibitors Interacting with Human Cyclophilin A

Meng Cui,[†,‡] Xiaoqin Huang,[†] Xiaomin Luo,[†] James M. Briggs,[‡] Ruyun Ji,[†] Kaixian Chen,[†] Jianhua Shen,*[,†] and Hualiang Jiang*[,†]

Center for Drug Discovery and Design, State Key Laboratory of Drug Research, Shanghai Institute of Materia Medica, Shanghai Institutes of Biological Sciences, Chinese Academy of Sciences, 294 Taiyuan Road, Shanghai 200031, P. R. China, and Department of Biology and Biochemistry, University of Houston, Houston, Texas 77204-5001

Received February 19, 2002

The interaction of a series gag peptide analogues with human cyclophilin A (hCypA) have been studied employing molecular docking and 3D-QSAR approaches. The Lamarckian Genetic Algorithm (LGA) and divide-and-conquer methods were applied to locate the binding orientations and conformations of the inhibitors interacting with hCypA. Good correlations between the calculated interaction free energies and experimental inhibitory activities suggest that the binding conformations of these inhibitors are reasonable. A novel interaction model was identified for inhibitors 11, 15, and 17 whose N-termini were modified by addition of the deaminovaline (Dav) group and the C-termini of 15 and 17 were modified by addition of a benzyl group. Accordingly, two new binding sites (sites A and D in Figure 1) were revealed, which show a strong correlation with inhibitor potency and thus can be used as a starting point for new inhibitor design. In addition, two predictive 3D-QSAR models were obtained by CoMFA and CoMSIA analyses based on the binding conformations derived from the molecular docking calculations. The reasonable r_{cross}^2 (cross-validated) values 0.738 and 0.762 were obtained for CoMFA and CoMSIA models, respectively. The predictive ability of these models was validated by four peptide analogues test set. The CoMFA and CoMSIA field distributions are in general agreement with the structural characteristics of the binding groove of hCypA. This indicates the reasonability of the binding model of the inhibitors with hCypA. Considering all these results together with the valuable clues of binding from references published recently, reasonable pharmacophore elements have been suggested, demonstrating that the 3D-QSAR models about peptide analogue inhibitors are expected to be further employed in predicting activities of the novel compounds for inhibiting hCypA.

Introduction

Cyclophilin A (CypA), a receptor of the immunosuppressive drug cyclosporin A (CsA),[1] catalyzes the cis−trans isomerization of peptidyl-prolyl bonds[2,3] and is required for the infectious activity of human immunodeficiency virus type 1 (HIV-1).[4−9] The gag of HIV is a polyprotein and cleaved by proteases into several functional proteins: matrix (MA), capsid (CA), nucleocapsid (NC), and small peptides.[10,11] The HIV CA protein is essential for the assembly and infectivity of HIV virions.[8,10,12,13] CypA binds directly to the CA domain of gag, with a CA−CypA stoichiometry of approximately 10:1 per virion.[5,6,14,15] Formation of the CA−CypA complex is competitively inhibited by molecules that bind at the active site of CypA, including the immunosuppressive drug cyclosporin and its nonimmunosuppressive analogue SDZ NIM 811.[4,16] This complex formation can also be inhibited by a series of mutations at the N-terminus of CA. Reagents and mutations that inhibit the CA−CypA interaction in vitro also block CypA packaging and HIV-1 replication in culture, demonstrating that this interaction is essential for viral infectivity.[5−7,17]

To investigate the mechanism by which CA and other reagents interact and recognize CypA, many three-dimensional structures of pure and in complex of human CypA (hCypA) have been determined.[18−31] These available crystal structures relative to CypA provided not only insights into the nature of CypA-gag interactions, but also valuable clues for designing new anti-AIDS drugs.[32,33] For example, crystal structures of cyclophilin A complexed with capsid protein and a binding site peptide or peptide analogue from the HIV-1 capsid protein[19,22−26] revealed two major interaction domains of CypA with peptides or peptide analogues. One domain is formed by the residues Phe60, Met61, Gln63, Ala101, Asn102 Ala103, Phe113, Leu122, and His126, the other one is formed by the residues Asn71, Gly72, and Thr73. Recently, Li et al. have designed and synthesized a series of gag peptide analogues with high inhibitory activities to hCypA, and one of them, a gag pentapeptide analogue, is more active than the entire capsid protein.[32] However, the crystal structure of this inhibitor in complex with hCypA is still not available. To investigate the mode of recognition and interaction mechanism of the gag peptide analogue inhibitors with hCypA, and to design new inhibitors with much higher inhibitory activities for hCypA, molecular docking and 3D-QSAR studies on these peptide analogues interacting with

* Corresponding authors. Phone: +86-21-64311833-222. Fax: +86−21−64370269. E-mail: jiang@iris3.simm.ac.cn or jhshen@mail.shcnc.ac.cn.
[†] Shanghai Institute of Materia Medica.
[‡] University of Houston.

10.1021/jm020082x CCC: $22.00
Published on Web 10/30/2002

Table 1. The Amino Acid Sequence, in Vitro Inhibitory Activities ($-\log IC_{50}$) of the Peptide Analogs, and the Predicted Binding Free Energies (ΔG, kcal/mol) with CypA from Molecular Docking Results

inhibitor	structure[a]	$IC_{50} \pm SD$ (μM)	$-\log IC_{50}$	ΔG (kcal/mol)
1	His-**Ala-Gly-Pro**-Ile-Ala	2000 ± 200	2.70 ± 0.04	-12.2
2	Ac-Val-His-**Ala-Gly-Pro**-Ile-Ala-NH_2	850 ± 220	3.07 ± 0.10	-13.8
3	Ac-Val-Gln-**Ala-Gly-Pro**-Ile-Ala-NH_2	2500	2.60 ± 0.00	-13.3
4	Ac-Val-His-**Ala-Gly-Pro**-Gly-Ala-NH_2	2800 ± 300	2.55 ± 0.04	-13.2
5	Ac-Val-His-**Ala-Gly-Pro**-Val-Ala-NH_2	1500 ± 300	2.82 ± 0.08	-13.6
6	Ac-Val-His-**Ala-Gly-Pro**-Gln-Ala-NH_2	1300 ± 200	2.89 ± 0.06	-13.4
7	Ac-Val-His-**Ala-Gly-Pro**-(L)phg-Ala-NH_2	820 ± 290	3.09 ± 0.13	-13.7
8	Ac-Val-His-**Ala-Gly-Pro**-(D)phg-Ala-NH_2	970 ± 400	3.01 ± 0.15	-13.6
9	Val-His-**Ala-Gly-Pro**-Ile-Ala-NH_2	2100 ± 300	2.68 ± 0.06	-13.5
10	Suc-Val-His-**Ala-Gly-Pro**-Ile-Ala-NH_2	1000 ± 800	3.00 ± 0.26	-15.1
11	Dav-His-**Ala-Gly-Pro**-Ile-Ala-NH_2	165 ± 70	3.78 ± 0.15	-16.2
12	Dah-**Ala-Gly-Pro**-Ile-Ala-NH_2	2600 ± 500	2.59 ± 0.08	-12.0
13	Ac-Val-His-**Ala-Gly-Pro**-Ile-NH-CH_2-Ph	115 ± 45	3.94 ± 0.14	-15.4
14	Ac-Val-His-**Ala-Gly-Pro**-Ile-NH-CH_2-CH_2-$(Ph)_2$	365 ± 155	3.44 ± 0.20	-16.7
15	Dav-His-**Ala-Gly-Pro**-Ile-NH-CH_2-Ph	6 ± 2	5.22 ± 0.12	-18.0
16	Ac-His-**Ala-Gly-Pro**-Ile-NH-CH_2-Ph	280 ± 100	3.55 ± 0.14	-14.3
17	Dav-His-**Ala-Gly-Pro**-Acp-NH-CH_2-Ph	90 ± 45	4.05 ± 0.18	-17.6
18	Dav-His-Aib-**Gly-Pro**-Acp-NH-CH_2-Ph	500 ± 130	3.30 ± 0.12	-15.0
19[b]	Ac-Val-His-**Ala-Gly-Pro**-Acp-Ala-NH_2	680 ± 180	3.17 ± 0.10	-13.6
20[b]	Ac-Val-His-Aib-**Gly-Pro**-Ile-Ala-NH_2	760 ± 310	3.12 ± 0.24	-15.1
21[b]	Val-His-**Ala-Gly-Pro**-Ile-NH-CH_2-Ph	260 ± 130	3.59 ± 0.18	-15.2
22[b]	Ac-Val-His-**Ala-Gly-Pro**-Ile-NH-CH_2-CH_2-Ph	325 ± 145	3.49 ± 0.21	-16.4

[a] The abbreviations Ac: acetyl; Acp: 2-aminocyclopentanecarboxylate; Aib: aminoisobutyric acid; Dah: deaminohistidine (dihydrourocanic acid); Dav: deaminovaline (isovaleric acid); Suc: succinyl; Ph: Phenyl; Phg: Phenylglycine. [b] Peptide analogues are selected for test set.

hCypA were performed, and predictive 3D-QSAR models have been constructed.

Computational Details

1. Molecular Structures and Optimization. A series of 22 gag peptide analogue inhibitors of human Cyclophilin A (hCypA), with the common central sequence of Ala(or Aib)-Gly-Pro synthesized by Li et al. recently,[32] were employed in this study (Table 1). The 1.58 Å resolution X-ray crystal structure of hCypA complexing with hexapeptide HAGPIA (PDB entry code 1AWQ, inhibitor **1** in Table 1)[23] was retrieved from the Brookhaven Protein Data Bank (PDB http://www.rcsb.org/pdb).[34] The structures of the gag peptide analogue inhibitors were constructed based on the structure of inhibitor **1** in the crystal structure 1AWQ[23] and energetically minimized using Tripos force field with Gasteiger−Hückel charges.[35] The AutoDock 3.0.3 program[36] was applied for flexibly docking these inhibitors into the binding site of hCypA. The complexes of these peptide analogues with hCypA resulted from molecular docking were further structurally optimized using molecular mechanics method with following parameters: the Amber4.0 force field,[37] Amber all-atom-charge and Powell method with the root-mean square (RMS) energy gradient of 0.08 kcal/(mol·Å), the whole system was minimized to convergence. Although the solvation energies were not explicitly considered during the minimization, the energy calculations were performed with a distance-dependent dielectric constant (ϵ) of 5 to simulate the solvation effect of the inhibitors in the protein environment.[38] The molecular modeling software Sybyl 6.8[39] was employed for CoMFA[40] and CoMSIA[41] analyses and visualization. All calculations were performed on Silicon Graphics O2 R12000 workstations.

2. Molecular Docking. To locate the appropriate binding orientations and conformations of these gag peptide analogue inhibitors interacting with hCypA, a powerful computational searching method is needed. The advanced molecular docking program AutoDock 3.0.3, which uses a powerful genetic algorithm (GA) method for conformational search and docking, was applied to perform the automated molecular docking simulations. To estimate the free energy of binding, an empirical free energy scoring function (eq 1) was applied in the docking calculations.

$$\Delta G = \Delta G_{vdw} + \Delta G_{hbond} + \Delta G_{elec} + \Delta G_{conf} + \Delta G_{tor} + \Delta G_{sol} \quad (1)$$

where the first four terms are the typical molecular mechanics terms for dispersion/repulsion, hydrogen-bonding, electrostatics, and deviations from covalent geometry, respectively; ΔG_{tor} models the restriction of internal rotors, global rotation, and translation; and ΔG_{sol} models the desolvation upon binding and the hydrophobic effects (solvent entropy changes at solute−solvent interfaces).[36]

The structures of hCypA and the peptide analogue inhibitors were prepared using the Sybyl 6.8[39] molecular modeling software. The Kollman all-atom-charge was assigned to hCypA according to Amber 4.0 force field. Atomic solvation parameters and fragmental volumes were assigned to hCypA using the Addsol module of the AutoDock program. The grid map with $121 \times 121 \times 121$ points and a spacing of 0.375 Å. was calculated using the Autogrid program, and was superimposed on the center of geometry of the inhibitor in the crystal structure. All hydrogen atoms were added to the peptide inhibitors; partial atomic charges were calculated using the Gasteiger−Marsili method.[35]

Residues Ala, Gly, and Pro of the inhibitor HAGPIA were conserved in many peptide inhibitors of hCypA, so they should be regarded as a critical motif for their inhibitory activities and/or the recognition by hCypA.[23,42] These residues are also conserved in the peptide analogue inhibitors in this study (Table 1), which indicates that they should adopt similar conformations upon binding to the same site of hCypA. The crystal structure of the complex demonstrated that, the Pro and Gly of HAGPIA "sitting" in a binding pocket (B) in the surface binding groove of hCypA (Figure 1a), could form six hydrogen bonds with hCypA (Figure 2a).[43] The H(487)A(488)G(489)P(490)I(491)A(492) segment in the crystal structure of Capsid−hCypA complex[19] was found in a similar mode as that of HAGPLA with hCypA. Therefore, the backbone conformation of the Ala-Gly-Pro (or Gly-Pro for peptide analogues 18 and 20) motif was initially restricted at early stage of molecular docking calculations according to the crystal structure of HAGPIA-hCypA complex. Then, a divide-and-conquer conformational search was performed, i.e., the torsion angles of each inhibitor, except those in the Ala-Gly-Pro segment, were subjected to the conformational search separately (Scheme 1). Thus, the final torsion angles subjected to conformational search were reduced to less than 10, which could be handled by the GA algorithm of AutoDock program. Also, since two parts of these inhibitors were found to be located in two binding sites of hCypA (Figure 1), the conformations of these

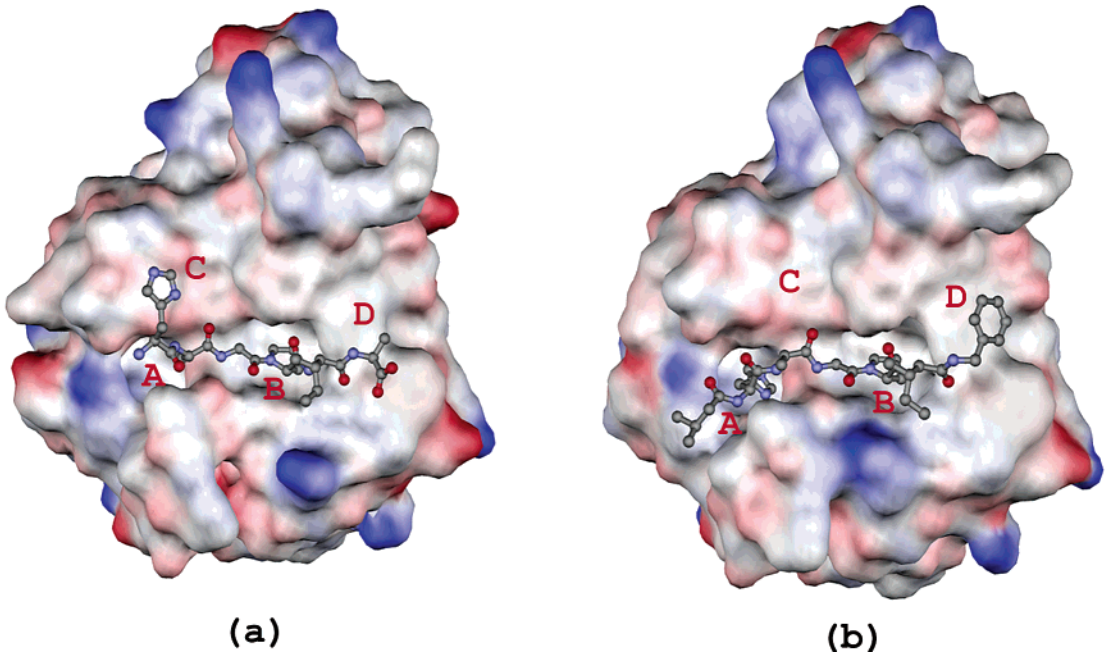

Figure 1. Binding models for HAGPIA (a) (crystal structure from PDB: 1AWQ) and inhibitor **15** (b) (docking structure) with hCypA. This image was generated with WebLab and rendered with POV−Ray. The CypA surface was colored by electrostatic potential.

two parts actually do not influence each other once the inhibitor bound with hCypA. Therefore, the docking search for the two "ends" of the inhibitors could be carried out separately for the sake of computation resource.

In this study, the Lamarckian Genetic Algorithm (LGA)[36] was selected to identify the binding conformations of the peptide analogue inhibitors. The step size was set to 0.2 Å for translation and 5° for orientation and torsion. Some important parameters for LGA calculations were reasonably set, i.e., an initial population of random individuals with a size of 50; a maximum number of 1.5×10^6 energy evaluations; a maximum number of generations of 2.7×10^4; an elitism value of 1, automatically surviving into the next generation; a mutation rate of 0.02, which was the probability that a gene would undergo a random change; and a crossover rate of 0.80, which was the probability proportional selection, was used, where the average of the worst energy was calculated over a window of the previous 10 generations; the pseudo-Solis and Wets local search method was used, having a maximum of 300 iterations per local search; the probability of performing local search on an individual in the population was 0.06; the maximum number of consecutive successes or failures before doubling or halving the local search step size, ρ, was 4, in both cases; and the lower bound on ρ, the termination criterion for the local search, was 0.01.

3. 3D-QSAR Studies. To more fully explore the specific contributions of electrostatic, steric and hydrophobic effects for these gag pentapeptide analogue inhibitors binding with hCypA, CoMFA,[41] and CoMSIA[42] studies were performed for these inhibitors based on the conformational alignment predicted from the molecular docking.

3.1. CoMFA. As usual, the steric and electrostatic field energies were probed using an sp^3 carbon atom and a +1 point charge, respectively. Steric and electrostatic interactions were calculated using the Tripos force field with a distance-dependent dielectic constant of 5 at all intersections in a regularly spaced (2 Å) grid. The minimum-sigma (column filtering) was set to 2.0 kcal/mol to improve the signal-to-noise ratio by omitting those lattice points whose energy variation was below this threshold. A cutoff of 30 kcal/mol was adopted, and the regression analysis was carried out using the partial least-squares (PLS) method. The final model was developed with the optimum number of components equal to that yielding the highest r_{cv}^2.

3.2. CoMSIA. Three physicochemical properties, namely steric, electrostatic and hydrophobic fields, have been evaluated. The steric contribution was reflected by the third power of the atomic radii of the atoms. Electrostatic properties were introduced as atomic charges resulted from molecular docking. An atom-based hydrophobicity was assigned according to the parametrization developed by Ghose et al.[44] The lattice dimensions were selected with a sufficiently large margin (>4 Å) to enclose all aligned molecules. Singularities were avoided at atomic positions in CoMSIA fields because a Gaussian-type distance dependence of the physicochemical properties was adopted, thus no arbitrary cutoffs were required. In general, similarity indices $A_{F,K}$ between the compounds of interest were computed by placing a probe atom at the intersections of the lattice points using eq 2,

$$A_{F,K}{}^{q}(j) = -\sum_{i=1}^{n} w_{probe,k} w_{ik} e^{-\alpha r_{iq}{}^2} \qquad (2)$$

where q represents a grid point; i is summation index over all atoms of the molecule j under computation; w_{ik} is the actual value of the physicochemical property k of atom i; $w_{prob,k}$ is the value of the probe atom. In present study, similarity indices were computed using a probe atom ($w_{probe,k}$) with charge +1, radius 1 Å, hydrophobicity +1, and attenuation factor α of 0.3 for the Gaussian-type distance. The statistical evaluation for the CoMSIA analyses was performed in the same way as described for CoMFA.

Results and Discussion

1. Interactions between Inhibitors and hCypA. 1.1 General Binding Mode. The automated molecular docking may produce several options of binding conformation for each inhibitor. The conformation corresponding to the lowest binding energy with hCypA was selected as the possible binding conformation. Thus the most probable binding conformations of the 22 peptide inhibitors (Table 1) were obtained. The 3D binding models for two typical inhibitors, **1** and **15**, are shown in Figure 1, and corresponding 2D interaction models

are presented in Figure 2. The molecular superposition of the binding conformations for these peptide analogue inhibitors extracted from the optimized inhibitor−hCypA complexes is shown in Figure 3.

From Figure 1, one can see that there are four binding sites in the surface binding groove of hCypA: site A is a small binding pocket formed by Lys82, Met100, Ala101, Asn102, Ala103, Thr107, Asn108, Gly109, Ser110, Gln111, and Phe112; near to site A, there is a larger pocket, which is called site B, formed by Phe60, Met61, Gln63, Ala101, Asn102 Ala103, Phe113, Leu122 and His126; site C is a shallow binding patch formed by Asn71, Gly72 and Thr73; and site D is formed by residues around Phe60. The molecular superposition of binding conformations (Figure 3) indicates that these peptide analogue inhibitors have a great part of similar interacting mode with CypA, especially for the conserved motif of these peptide analogue inhibitors, "Ala-Gly-Pro", it fits geometrically well with site B and the "saddle" linking sites A and B (Figure 1), and forms several hydrogen-bonds with residues Arg55, Gln63, Gly72, and Trp121 of hCypA (Figures 1, 2), which looks like the mode of HAGPIA interacting with hCypA revealed by the crystal structure 1AWQ. On the other hand, some differences in binding also exist, inhibitors **2**−**10**, **12**, and **19** adopt almost the same interaction mode with inhibitor **1** (Figure 1a) and occupy most part of binding sites B and C, while inhibitors **11**, **15**, and **17** locate mainly at sites A, B, and D (Figure 1b), the Dav-His moiety at the N-terminus (Figures 2, 3) interacts with the side chains of residues situated in the hydrophobic pocket A (Figures 1b, 2b).

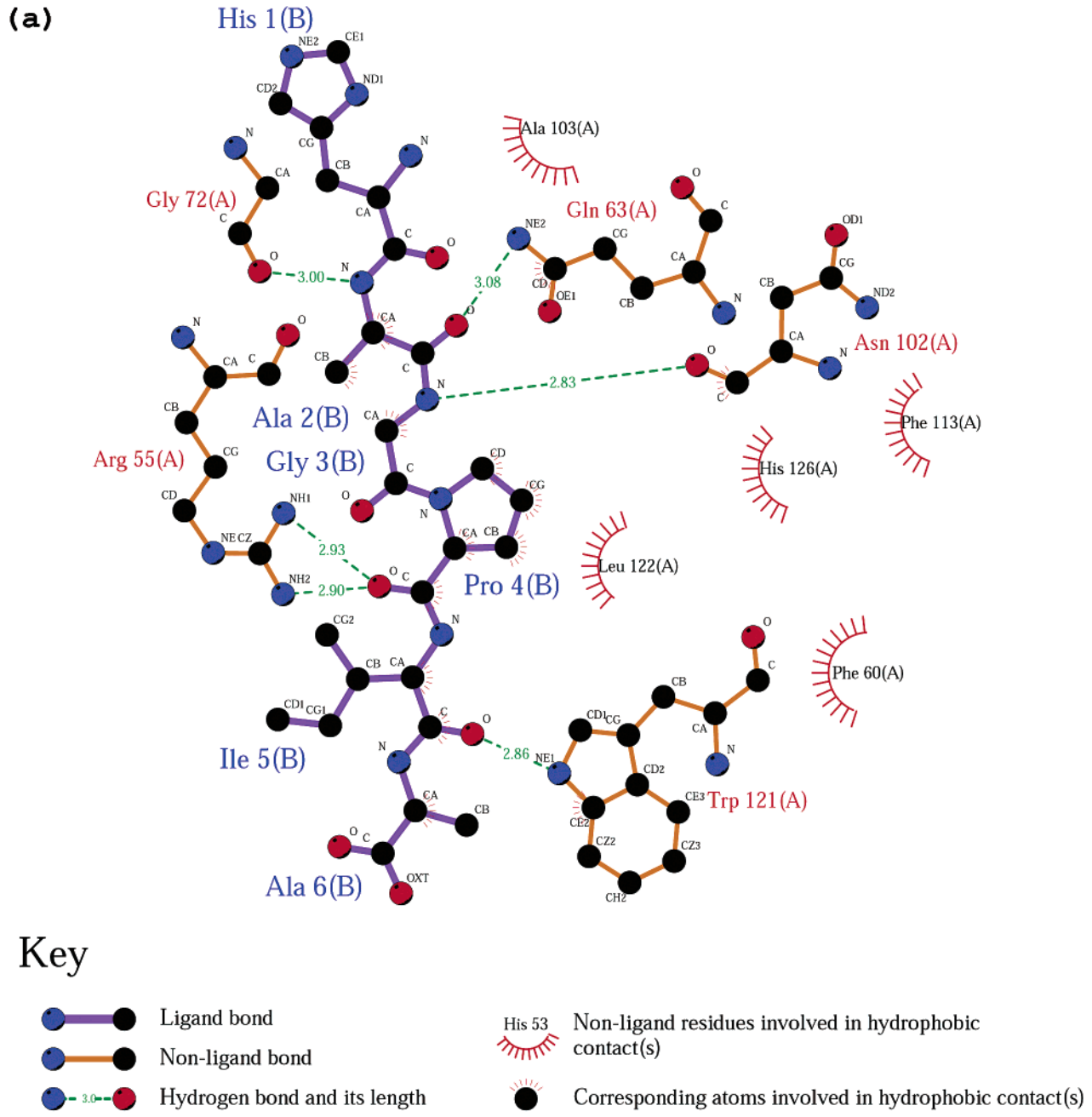

Figure 2. Schematic depiction of the main interactions of HAGPIA (a) and inhibitor **15** (b) with hCypA (crystal structure from PDB: 1AWQ). This image was generated with LIGPLOT program.[43] A distance between donor and acceptor of less than 3.4 Å is considered as a hydrogen-bond, and a 4.1 Å distance between two hydrophobic atoms is considered a hydrophobic interaction.

Figure 2 (Continued)

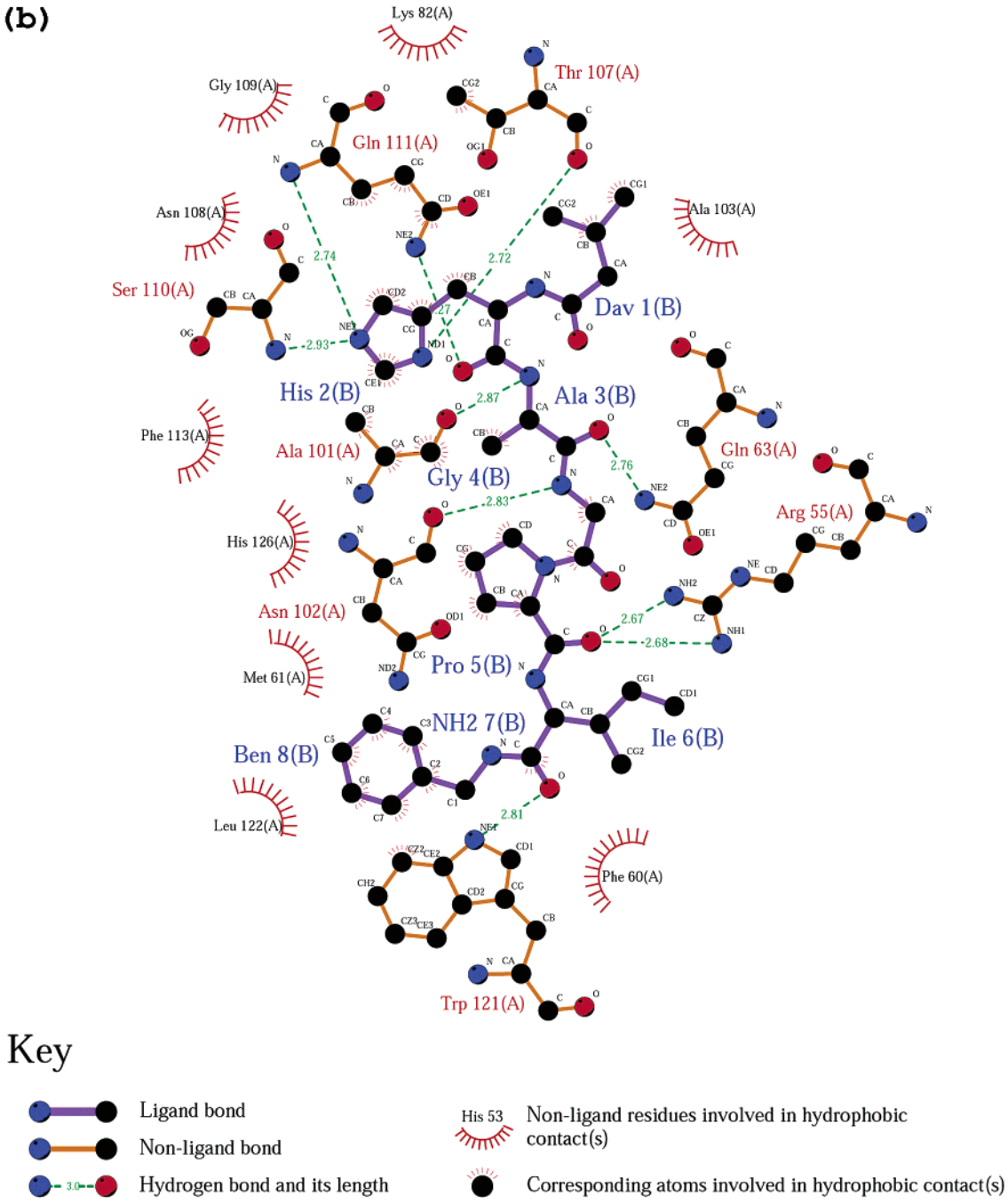

To illustrate the interaction mechanism, inhibitor **15**, the most potent peptide analogue inhibitor with highest inhibitory activity, was selected for more detailed analyze. The intermolecular hydrogen-bonds and hydrophobic contacts between **15** and hCypA are summed in Tables 2 and 3, respectively. In comparison with inhibitor **1** (Figures 1a and 2a), inhibitor **15** retains the six hydrogen-bonds (Figure 2b), viz. two hydrogen-bonds of Ala with Gln63 and Ala101; two hydrogen-bonds of Pro with Arg55; one between Ile and Trp121; and one between Gly and Asn102. In addition, four extra hydrogen-bonds are formed by the N-terminus of inhibitor **15** with site A, three of them formed between the side chain of residue His of **15** with residues Ser110 and Gln111 of hCypA; the backbone carbonyl group of His of **15** forms another H-bond with Gln111. Furthermore, hydrophobic interactions between **15** and hCypA are more potent than that of inhibitor **1**, besides the common hydrophobic interactions of Pro with side chains of residues at site B of hCypA, more extensive hydrophobic contacts exist between the N-terminus of **15** and the side chains of residues Lys82, Ala101, Asn108, Gly109, and Gln111 at site **A** of hCypA. Additionally, the benzyl group at C-terminus of **15** hydrophobically interacts with the side chains of residues Phe60 and Trp121 of hCypA.

1.2. Novel Binding Sites. The docking results demonstrate that sites A and D are the novel and very important binding sites that have not been previously appreciated, because they have not been revealed in the

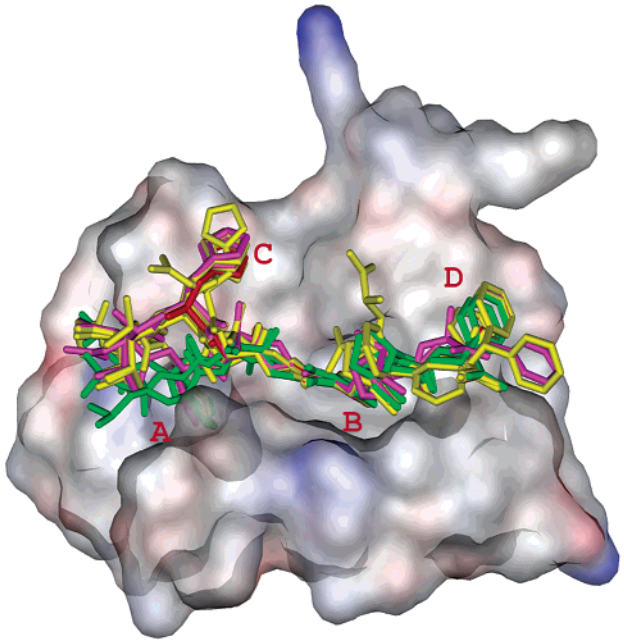

Figure 3. Probable binding conformations of the peptide analogue inhibitors resulting from molecular docking and their superpositions in the binding groove of hCypA (inhibitor1 is colored red; inhibitors 11, 15, and 17 are colored green; inhibitors 2−10, 12−14, 16, and 18 are colored yellow; inhibitors 19−22 are colored magenta). The CypA surface was colored by electrostatic potential. A, B, C, and D respectively correspond to the four binding sites A−D in hCypA (see Figure 1). This image was rendered by the POV−Ray program.

Scheme 1. The Indicated Rotatable Bonds of Ligand 13 Were Treated as Rotatable during Molecular Docking. The Central Domain, Ala-Gly-Pro, Was Restricted According to the Conformation Encoded in the HAGPIA−hCypA Complex (1AWQ); the Left and Right Side Rotatable Bonds Were Calculated Separately during the Docking Simulations.

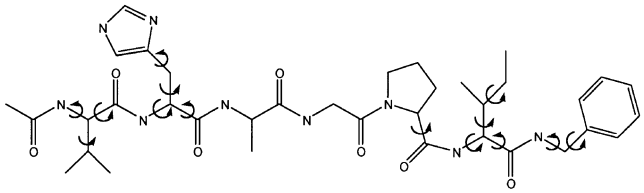

Table 2. The Hydrogen-Bonds Formed between the Inhibitor **15** and HCypA

15		hCypA		
residue	atom	residue	atom	distance (Å)
His2	O	Gln111	NE2	3.27
His2	NE2	Gln111	N	2.74
His2	NE2	Ser110	N	2.93
His2	ND1	Thr107	O	2.72
Ala3	N	Ala101	O	2.87
Ala3	O	Gln63	NE2	2.76
Gly4	N	Asn102	O	2.83
Pro5	O	Arg55	NH2	2.67
Pro5	O	Arg55	NH1	2.68
Ile6	O	Trp121	NE1	2.81

available X-ray crystal structures of peptide−CypA complexes.[19,22−26,45] This may rationalize why inhibitors **11**, **15**, and **17** are more active than the other inhibitors.[32] Binding free energy calculations also indicate that these three inhibitors have higher binding affinities than the others (Table 1 and the following discussion).

Table 3. The Hydrophobic Contacts between the Inhibitor **15** and HCypA

inhibitor **15**		hCypA		
residue	atom	residue	atom	distance(Å)
Dav1	CB	Trp107	CG2	3.77
Dav1	CG1	Trp107	CG2	3.85
His2	CD2	Lys82	CE	3.86
His2	CG	Lys82	CE	3.88
His2	CB	Lys82	CE	3.29
His2	CE1	Ala101	C	3.75
His2	CE1	Asn108	C	3.69
His2	CE1	Asn108	CA	3.68
His2	CE1	Gly109	CA	3.80
His2	CD2	Gly109	CA	3.72
His2	CD2	Gln111	CD	3.86
His2	CD2	Gln111	CG	3.47
His2	CE1	Gln111	CB	3.87
His2	CD2	Gln111	CB	3.55
Ala3	CB	Ala103	CB	3.73
Gly4	CA	Ala101	CB	3.57
Gly4	CA	Ala101	C	3.66
Gly4	CA	Ala101	CA	3.69
Gly4	C	His126	CE1	3.59
Pro5	CG	Met61	SD	3.81
Pro5	CG	Phe113	CZ	3.87
Pro5	CG	Phe113	CE1	3.87
Pro5	CD	Phe113	CD1	3.75
Pro5	CG	Phe113	CD1	3.86
Pro5	CG	Phe113	CG	3.85
Pro5	CB	Leu122	CD2	3.42
Pro5	CB	Leu122	CD1	3.45
Pro5	CA	His126	CE1	3.75
Ile6	C	Phe60	CZ	3.52
Ben8	C7	Phe60	CE2	3.83
Ben8	C2	Phe60	CE2	3.89
Ben8	C6	Phe60	CD2	3.56
Ben8	C5	Phe60	CD2	3.43
Ben8	C4	Phe60	CD2	3.68
Ben8	C4	Phe60	CD1	3.73
Ben8	C5	Phe60	CG	3.56
Ben8	C4	Phe60	CG	3.44
Ben8	C5	Phe60	CB	3.69
Ben8	C4	Phe60	CB	3.75
Ben8	C3	Trp121	CZ2	3.76

The binding models from the docking simulations revealed a clear picture of the structure−activity relationship for the 22 inhibitors. Adding the Dav group to the N-terminus of inhibitor **1** makes the His in inhibitors **11**, **15**, and **17** fit into site **A**, forming more favorable hydrogen-bonds and hydrophobic interaction contacts as mentioned above. These additional interactions increase the binding affinity for inhibitors **11**, **15**, and **17** with hCypA, and thus the inhibitory activity. Modifying the C-terminus with a benzyl group increases hydrophobic interaction contacts for the inhibitors with site D of hCypA greatly. These two end modifications respectively by Dav-His and a benzyl group facilitate the inhibitors binding with hCypA using the two new binding sites, sites A and D, which not only increase the hydrogen bonds and the hydrophobic interacting pairs, but also serve as two "clamps" to anchor the two ends of the inhibitors at sites A and D and constrain their conformational flexibility in the complex with hCypA. The two new binding sites increase the inhibitory activities of inhibitors **15** and **17** about 200−300 times higher than that of inhibitor **1** and even more potent than the entire HIV-1 capsid protein.[32]

2. The Correlation between Binding Free Energy and Inhibitory Activity. The predicted binding free energies of these peptide analogue inhibitors bind-

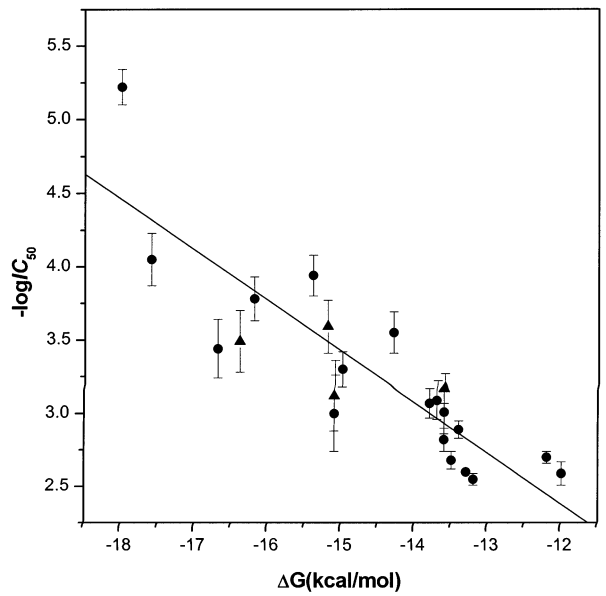

Figure 4. Correlation between the binding free energies (ΔG, kcal/mol, $T = 298.15$ K) of the peptide analogue inhibitors with the hCypA and the experimental activities ($-\log IC_{50}$). ●, peptide analogue inhibitors of the training set; ▲, peptide analogue inhibitors of the testing set.

ing to hCypA are also listed in Table 1. Satisfied that the binding models of the peptide analogue inhibitors with hCypA were indeed reasonable, we then performed a linear regression analysis to explore whether the inhibitory activities of the peptide analogues could be correlated with the energetic parameters. By using experimentally determined IC_{50} values (the same protein concentrations for human CypA (16 nm) were used)[32] (Table 1) and employing linear analysis, we calculated the regression equation for the inhibitory activities, $-\log IC_{50}$, using the total binding free energies, ΔG, as the sole descriptor variable. A good correlation was found between the inhibitory activities and the predicted binding free energies (eq 3), and this relationship is graphically shown in Figure 4. The relationship suggests that those potential analogue peptide inhibitors exhibiting stronger binding free energies using this paradigm would, therefore, be expected to have greater efficacy toward inhibitory action. This good correlation further demonstrates the reasonability of the binding conformations and binding models for the peptide inhibitors with hCypA.

$$-\log IC_{50} = -1.778 - 0.346\Delta G \qquad (2)$$

$$(n = 18,\ r^2 = 0.772,\ F = 54.313,\ s = 0.335)$$

On the basis of the binding free energies and their correlation with the inhibitory activities, we can give a more quantitative explanation to the structure−activity relationship of the inhibitory mechanism for these inhibitors. It is obvious that there would be nearly a 1.4 kcal/mol difference in binding free energy if there is 1 order of magnitude for numerical difference in the inhibitory potency (IC_{50}). As listed in Table 1, the increased value of the binding free energy of 2.5 kcal/mol for inhibitor **11** caused by substitutions at the N-terminus of inhibitor **2** from His to Dav-His can be assigned the additional interactions of Dav-His with site **A** (Figures 1−3). As discussed above, inhibitors **13**, **15**, and **17** have an additional hydrophobic interaction between the phenyl group and the benzene ring of Phe60, which may increase the binding affinity by 1.3−1.7 kcal/mol, as indicated in Table 1.

Table 4. Statistical Indexes of CoMFA and CoMSIA Models Based on Peptide Analog Inhibitors Binding Conformations

	cross-validated		conventional		
	r_{cross}^2	optimal comp.	r^2	s	F
CoMFA	0.738	3	0.979	0.109	216.150
CoMSIA	0.762	5	0.989	0.084	221.112
	Field Distribution (%)				
steric		53.9		17.3	
electrostatic		46.1		21.4	
hydrophobic				17.2	
H-bond donor				25.9	
H-bond acceptor				18.2	

Table 5. Predicted Activities (PA) from CoMFA and CoMSIA Models Compared with the Experimental Activities (EA) and the Residuals (δ)

inhibitor	CoMFA			CoMSIA	
	EA	PA	δ	PA	d
1	2.70	2.67	0.03	2.70	0.00
2	3.07	2.98	0.09	3.02	0.05
3	2.60	2.57	0.03	2.57	0.03
4	2.55	2.71	−0.16	2.70	−0.15
5	2.82	2.86	−0.04	2.92	−0.10
6	2.89	2.89	−0.00	2.87	0.02
7	3.09	2.91	0.18	3.03	0.06
8	3.01	3.07	−0.06	2.87	0.02
9	2.68	2.76	−0.08	2.68	0.00
10	3.00	2.91	0.09	3.06	−0.06
11	3.78	3.71	0.07	3.77	0.01
12	2.59	2.54	0.05	2.59	0.00
13	3.94	3.79	0.15	3.79	0.15
14	3.44	3.61	−0.17	3.46	−0.02
15	5.22	5.20	0.02	5.31	−0.09
16	3.55	3.69	−0.14	3.46	0.09
17	4.05	4.04	0.01	4.02	0.03
18	3.30	3.35	−0.05	3.34	−0.04
19[a]	3.17	3.13	0.04	3.03	0.14
20[a]	3.12	3.22	−0.10	3.34	−0.22
21[a]	3.59	3.60	−0.01	3.52	0.07
22[a]	3.49	3.36	0.13	3.41	0.08

[a] Peptide analogues are selected for test set.

3. CoMFA and CoMSIA Analyses. 3.1. CoMFA. Although CoMFA is not able to appropriately describe all aspects of the binding forces, being based principally on standard steric and electrostatic molecular fields to model substrate−enzyme interactions, it is still a widely used tool for the study of QSAR at the 3D level. The major objective of CoMFA analysis for the peptide analogue inhibitors is to find the best predictive model within the system. We picked up the first 18 peptide analogue inhibitors for CoMFA analyses, the other four as testing compounds for the model validations. PLS analysis results based on least-squares fitting are listed in Table 4, which shows that all of the statistical indexes are reasonably high. The predicted activities of the 18 peptide analogue inhibitors from the 3D-QSAR model versus their experimental inhibitory activities ($-\log IC_{50}$) are compiled in Table 5. As listed in Table 4, a CoMFA model with r_{cross}^2 value of 0.738 for three components, and conventional r^2 of 0.979, are obtained based on the binding conformations and their alignment in the active site of hCypA. The linear relationship

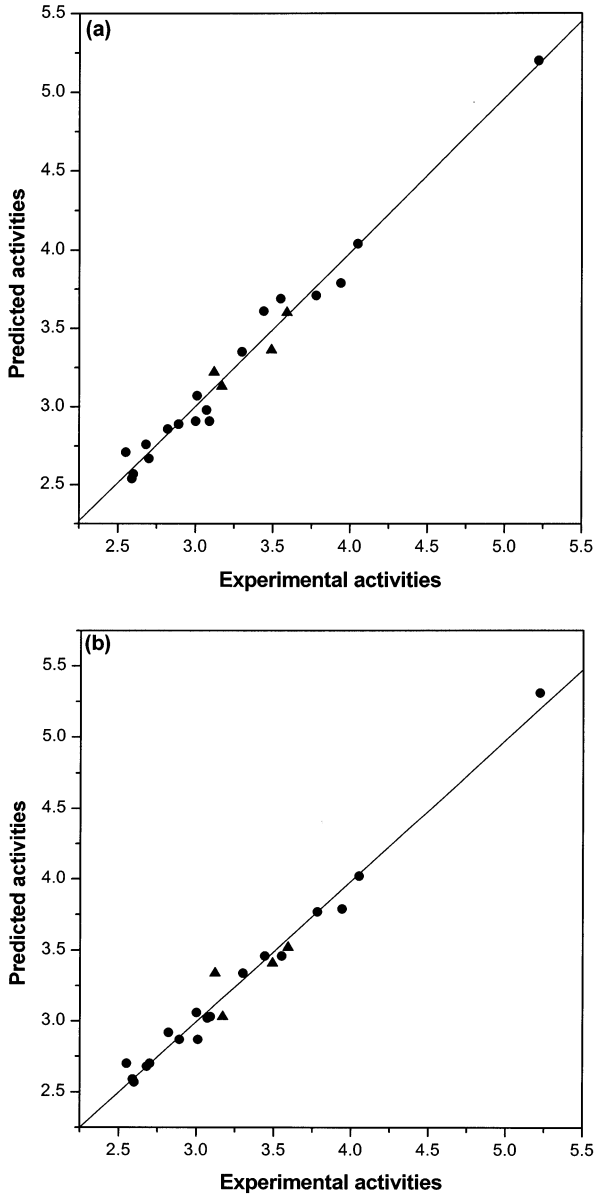

Figure 5. Predicted activities (PA) by CoMFA (a) and CoMSIA (b) models versus experimental activities (EA) of peptide analogue inhibitors. ●, peptide analogue inhibitors of the training set; ▲, peptide analogue inhibitors of the testing set.

shown in Figure 5a indicates that the fitting power is phenomenal and the predictive ability is good.

The CoMFA map is illustrated in Figure 6a. Colored polyhedra in the map show these areas in 3D space where changes in the field values for peptide inhibitors correlate strongly with concomitant changes in inhibitory activities. Detrimental and beneficial steric interactions are respectively displayed in yellow and green contours, while blue and red contours illustrate the regions of desirable positive and negative electrostatic interactions.

Several insights into the binding of the peptide analogue inhibitors can be readily observed from the CoMFA map. First, a large region of green contour around the C-terminus of these inhibitors suggests that more bulky substituents in these positions will significantly improve the biological activities. Since many bulky groups such as *tert*-butyl, cyclohexyl, and phenyl are hydrophobic, they may also be able to take advantage of the hydrophobic nature of site D in binding (Figures 1b, 2b, and 3). Indeed, substitution of the C-terminus of an inhibitor by a bulky group, such as benzyl (inhibitors **11**, **15**, and **17**), exhibited a considerable gain in binding affinity due to the increased hydrophobic interaction between the C-terminus and the environment around Phe60 (site D). The yellow polyhedra above both N-terminus and C-terminus of the inhibitors indicate that increased steric bulk is unfavorable for the inhibitory activities. This is also quite complementary with the model structures of inhibitor−hCypA complexes. Adding more bulky groups around the yellow polyhedron at the C-terminus may bring steric clash of these inhibitors with the side chain of Arg148 of hCypA, or the substituted bulky groups at these two yellow polyhedra have to be exposed to solvent; neither of these situations are beneficial to the inhibitor−hCypA binding. The blue contours near the region of the His in inhibitor **15** suggest that positively charged substituents may increase the inhibitory activity. This electrostatic field is complementary with the electrostatic interaction of His with site A (Figures 1 and 3). Therefore, we conclude that the CoMFA fields generated from AutoDock aligned conformations have reasonably described the structure of the binding groove of hCypA.

3.2. CoMSIA. CoMSIA analysis results are also summarized in Table 4. A CoMSIA model with an r_{cross}^2 value of 0.762 for five components and conventional r^2 of 0.989 was obtained. These data demonstrate that the CoMSIA model is also fairly predictive. The predicted inhibitory activities of peptide analogue inhibitors are listed in Table 5 and also shown in Figure 5. The high value of the conventional r^2 relating to five different descriptor variables (steric, electrostatic, hydrophobic, hydrogen-bond donor and acceptor; Table 4) illustrate that these variables are necessary to describe the field properties around the peptide analogue inhibitors, as well as the interaction mode of these peptide inhibitors with hCypA. The CoMSIA map is illustrated in Figure 6b. Colored polyhedra in the map represent the beneficial hydrophobic interaction regions which are displayed in green, while the desirable hydrophilic interaction regions are illustrated in white.

The yellow contours around the C terminus of peptide analogues, and the region between sites C and D suggest that the hydrophobic groups are favorable for increasing activity. The benzyl group of the C-terminus and the side chain of the Ile residue in inhibitor **15** indicate that more hydrophobic group substitutions will increase the inhibitory activity of the peptide analogue inhibitors. The white contours around the upper region of site A indicate that the backbones of favorable conformations of peptide analogues may occupy this area; and the upper region of site D indicates the hydrophilic groups are favorable because it is exposed to the solvent. The cyan and magenta contours around the site A indicate that hydrogen-bond donors and acceptors are favorable in this area, respectively. This is in agreement with the inhibitor-protein binding model. As hydrogen-bond acceptors, residues Ala101, Thr107, and Gln111 of site A hydrogen-bond with the side chain of residue His and the backbone of some peptide analogues; while residues

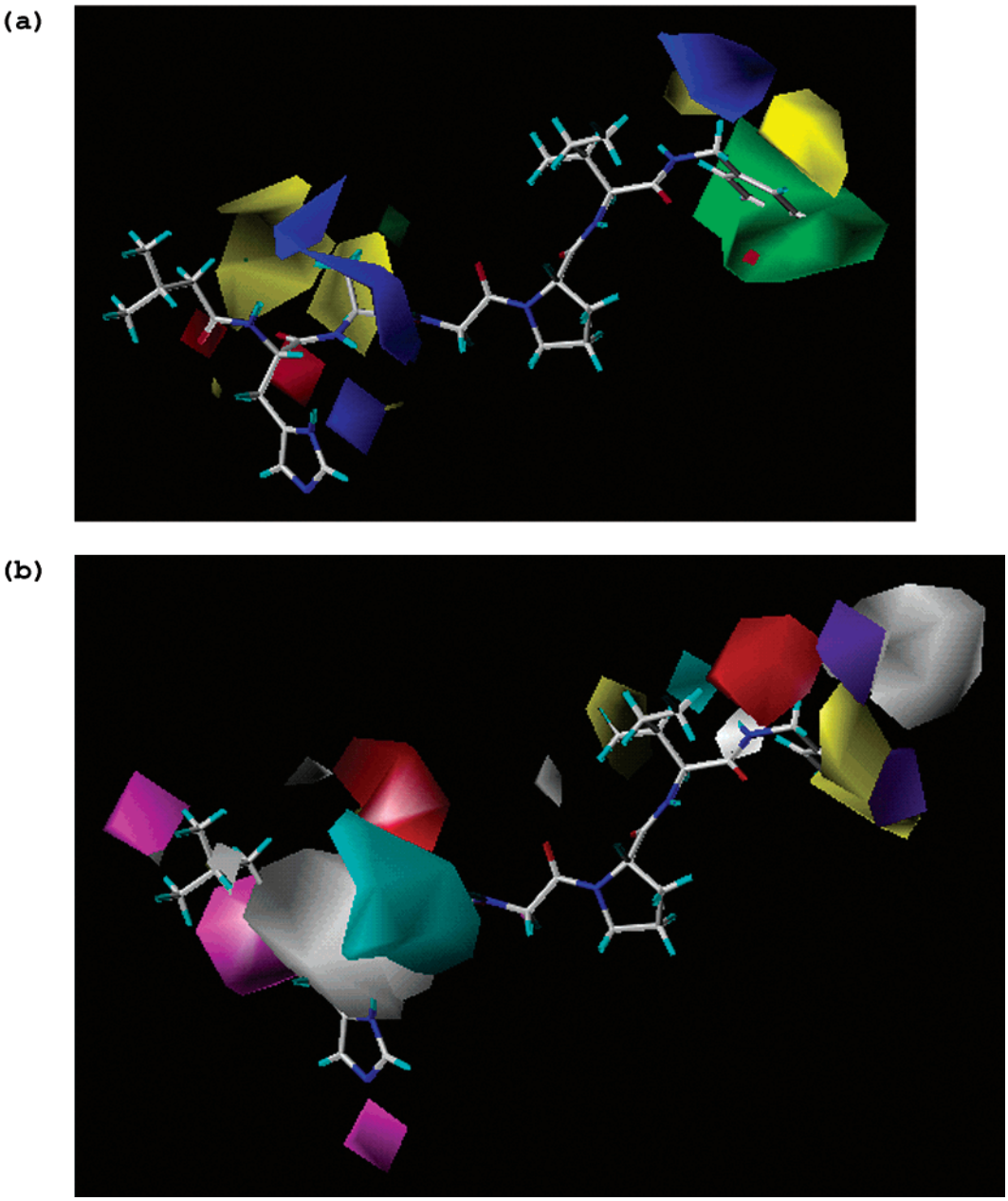

Figure 6. (a) CoMFA contour map. Sterically favored areas (contribution level of 80%) in green. Sterically unfavored areas (contribution level 20%) in yellow. Positive-charge-favored areas (contribution level 80%) in blue. Positive-charge-unfavored areas (contribution level of 20%) in red. (b) CoMSIA contour map. Hydrophobic favored areas (contribution level of 80%) in yellow; hydrophobic unfavored areas (contribution level of 20%) in white. Hydrogen-bond-donor-favored areas (contribution level of 80%) in cyan; hydrogen-bond-donor-unfavored areas (contribution level of 20%) in purple. Hydrogen-bond-acceptor-favored areas (contribution level of 80%) in magenta; hydrogen-bond-acceptor-unfavored areas (contribution level of 20%) in red.

Ser110, Gln111 of the site A form hydrogen-bonds with the side chain of the residue His and the backbone of some favorable peptide analogues as hydrogen-donors (Figures 1−3).

3.3. Validation of the 3D-QSAR Models. To validate our models, four peptide analogue inhibitors (19 to 22 in Table 1) that were not included in generating CoMFA and CoMSIA models were selected as testing compounds. The results are simultaneously shown in Table 5 (star labeled) and Figure 5 (in triangle symbols). The predicted $-\log IC_{50}$ values are in good agreement with the experimental data in a statistically tolerable error range, $r^2 = 0.979$ and 0.989 for CoMFA and CoMSIA models, respectively. The testing results for the four peptide analogue inhibitors indicate that the CoMFA and CoMSIA models can be further used in new peptide analogue inhibitors design for hCypA.

4. Pharmacophore Elements. Taking into account of the interaction mechanism of peptide analogue inhibitors with hCypA (Figures 1−3) and indications from the stable and predictive 3D-QSAR models (Figure 6), 3D-pharmacophore elements of these inhibitors against hCypA could be logically figured out. As shown in Figure 7, the 3D-pharmacophore is composed by two different types of interacting mode of the inhibitors with hCypA (inhibitors **1** and **15** as the two typical examples) and the binding sites A−D. The geometric parameters indicating the space distances between several active groups, which are also shown in Figure 7, may be used in database searching for new inhibitor discovery.

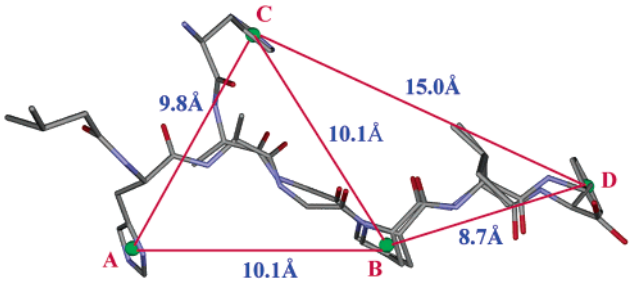

Figure 7. Pharmacophore elements for peptide analogue inhibitors binding with hCypA.

Conclusions

In summary, we have predicted the binding conformations of a series of 22 peptide analogue inhibitors against hCypA employing automated molecular docking program, Autodock 3.0.3. Results from LGA algorithm indicate that the binding free energies of these inhibitors correlate well with their reported inhibitory activities, and the calculation results provide a satisfactory explanation for the binding mechanism of the studied compounds. Most importantly, two novel binding sites, site A and site D, situated in the binding groove of hCypA, were for the first time revealed by our molecular docking simulations (Figure 1b). The higher binding affinities of the more potent inhibitors **11**, **15**, and **17** may contributed to the additional hydrophobic interactions and hydrogen bonding with these two newly uncovered binding sites.

Furthermore, CoMFA and CoMSIA studies were performed based on the molecular superposition of these peptide analogue inhibitors, and predictive 3D-QSAR models have been constructed. The CoMFA and CoMSIA field distributions are in agreement with the structural features of the active site of hCypA. Therefore, the CoMFA and CoMSIA models, together with the application of the valuable clues from pharmacophore elements, are expected to be fast and convenient tools to design new peptide analogue inhibitors with higher inhibitory activities against hCypA.

Acknowledgment. The authors thank Professor Arthur J. Olson for his kindness in offering us the AutoDock 3.0.3 program. We gratefully acknowledge financial support from National Natural Science Foundation of China (grants 29725203 and 20072042), the State Key Program of Basic Research of China (grant 1998051115), Life Science Foundation for Young Scientists of CAS (grant STZ-00-06), Qi Ming Xing Foundation of Shanghai Ministry of Science and Technology (grant 00QB14034), and Postdoctoral Fellowship of Shanghai.

References

(1) Handschumacher, R. E.; Harding, M. W.; Rice, J.; Drugge, R. J.; Speicher, D. W. Cyclophilin: a specific cytosolic binding protein for cyclosporin A. *Science* **1984**, *226*, 544−547.
(2) Fischer, G.; Wittmann-Liebold, B.; Lang, K.; Kiefhaber, T.; Schmid, F. X. Cyclophilin and peptidyl-prolyl cis−trans isomerase are probably identical proteins. *Nature* **1989**, *337*, 476−478.
(3) Takahashi, N.; Hayano, T.; Suzuki, M. Peptidyl-prolyl cis−trans isomerase is the cyclosporin A-binding protein cyclophilin. *Nature* **1989**, *337*, 473−475.
(4) Luban, J.; Bossolt, K. L.; Franke, E. K.; Kalpana, G. V.; Goff, S. P. Human immunodeficiency virus type 1 Gag protein binds to cyclophilins A and B. *Cell* **1993**, *73*, 1067−1078.
(5) Franke, E. K.; Yuan, H. E.; Luban, J. Specific incorporation of cyclophilin A into HIV-1 virions. *Nature* **1994**, *372*, 359−362.
(6) Thali, M.; Bukovsky, A.; Kondo, E.; Rosenwirth, B.; Walsh, C. T. et al. Functional association of cyclophilin A with HIV-1 virions. *Nature* **1994**, *372*, 363−365.
(7) Braaten, D.; Franke, E. K.; Luban, J. Cyclophilin A is required for the replication of group M human immunodeficiency virus type 1 (HIV-1) and simian immunodeficiency virus SIV(CPZ)-GAB but not group O HIV-1 or other primate immunodeficiency viruses. *J. Virol.* **1996**, *70*, 4220−4227.
(8) Freed, E. O. HIV-1 gag proteins: diverse functions in the virus life cycle. *Virology* **1998**, *251*, 1−15.
(9) Braaten, D.; Luban, J. Cyclophilin A regulates HIV-1 infectivity, as demonstrated by gene targeting in human T cells. *EMBO J.* **2001**, *20*, 1300−1309.
(10) Wills, J. W.; Craven, R. C. Form, function, and use of retroviral gag proteins. *Aids* **1991**, *5*, 639−654.
(11) Gelderblom, H. R. Assembly and morphology of HIV: potential effect of structure on viral function. *Aids* **1991**, *5*, 617−637.
(12) Braaten, D.; Ansari, H.; Luban, J. The hydrophobic pocket of cyclophilin is the binding site for the human immunodeficiency virus type 1 Gag polyprotein. *J. Virol.* **1997**, *71*, 2107−2113.
(13) Dorfman, T.; Weimann, A.; Borsetti, A.; Walsh, C. T.; Gottlinger, H. G. Active-site residues of cyclophilin A are crucial for its incorporation into human immunodeficiency virus type 1 virions. *J. Virol.* **1997**, *71*, 7110−7113.
(14) Franke, E. K.; Luban, J. Cyclophilin and gag in HIV-1 replication and pathogenesis. *Adv. Exp. Med. Biol.* **1995**, *374*, 217−228.
(15) Ott, D. E.; Coren, L. V.; Johnson, D. G.; Sowder, R. C., 2nd; Arthur, L. O. Henderson, L. E. Analysis and localization of cyclophilin A found in the virions of human immunodeficiency virus type 1 MN strain. *AIDS Res. Hum. Retroviruses* **1995**, *11*, 1003−1006.
(16) Billich, A.; Hammerschmid, F.; Peichl, P.; Wenger, R.; Zenke, G.; Quesniaux, V.; Rosenwirth, B. Mode of action of SDZ NIM 811, a nonimmunosuppressive cyclosporin A analogue with activity against human immunodeficiency virus (HIV) type 1: interference with HIV protein-cyclophilin A interactions. *J. Virol.* **1995**, *69*, 2451−2461.
(17) Steinkasserer, A.; Harrison, R.; Billich, A.; Hammerschmid, F.; Werner, G. Wolff, B.; Peichl, P.; Palfi, G.; Schnitzel, W.; Mlynar, E. Mode of action of SDZ NIM 811, a nonimmunosuppressive cyclosporin A analogue with activity against human immunodeficiency virus type 1 (HIV-1): interference with early and late events in HIV-1 replication. *J. Virol.* **1995**, *69*, 814−824.
(18) Mikol, V.; Kallen, J.; Pflugl, G.; Walkinshaw, M. D. X-ray structure of a monomeric cyclophilin A-cyclosporin A crystal complex at 2.1 A resolution. *J. Mol. Biol.* **1993**, *234*, 1119−1130.
(19) Gamble, T. R.; Vajdos, F. F.; Yoo, S.; Worthylake, D. K.; Houseweart, M. Sundquist, W. I.; Hill, C. P. Crystal structure of human cyclophilin A bound to the amino-terminal domain of HIV-1 capsid. *Cell* **1996**, *87*, 1285−1294.
(20) Ke, H. M.; Zydowsky, L. D.; Liu, J.; Walsh, C. T. Crystal structure of recombinant human T-cell cyclophilin A at 2.5 A resolution. *Proc. Natl. Acad. Sci. U. S. A.* **1991**, *88*, 9483−9487.
(21) Ke, H. Similarities and differences between human cyclophilin A and other beta-barrel structures. Structural refinement at 1.63 A resolution. *J. Mol. Biol.* **1992**, *228*, 539−550.
(22) Zhao, Y.; Ke, H. Mechanistic implication of crystal structures of the cyclophilin-dipeptide complexes. *Biochemistry* **1996**, *35*, 7362−7368.
(23) Vajdos, F. F.; Yoo, S.; Houseweart, M.; Sundquist, W. I.; Hill, C. P. Crystal structure of cyclophilin A complexed with a binding site peptide from the HIV-1 capsid protein. *Protein Sci.* **1997**, *6*, 2297−2307.
(24) Zhao, Y.; Chen, Y.; Schutkowski, M.; Fischer, G.; Ke, H. Cyclophilin A complexed with a fragment of HIV-1 gag protein: insights into HIV-1 infectious activity. *Structure* **1997**, *5*, 139−146.
(25) Kallen, J.; Walkinshaw, M. D. The X-ray structure of a tetrapeptide bound to the active site of human cyclophilin A. *FEBS Lett.* **1992**, *300*, 286−290.
(26) Ke, H.; Mayrose, D.; Cao, W. Crystal structure of cyclophilin A complexed with substrate Ala-Pro suggests a solvent-assisted mechanism of cis−trans isomerization. *Proc. Natl. Acad. Sci. U. S. A.* **1993**, *90*, 3324−3328.
(27) Ke, H.; Mayrose, D.; Belshaw, P. J.; Alberg, D. G.; Schreiber, S. L. Chang, Z. Y.; Etzkorn, F. A.; Ho, S.; Walsh, C. T.. Crystal structures of cyclophilin A complexed with cyclosporin A and *N*-methyl-4-[(E)-2-butenyl]-4,4-dimethylthreonine cyclosporin A. *Structure* **1994**, *2*, 33−44.
(28) Mikol, V.; Kallen, J.; Walkinshaw, M. D. X-ray structure of a cyclophilin B/cyclosporin complex: comparison with cyclophilin A and delineation of its calcineurin-binding domain. *Proc. Natl. Acad. Sci. U. S. A.* **1994**, *91*, 5183−5186.

(29) Pflugl, G.; Kallen, J.; Schirmer, T.; Jansonius, J. N.; Zurini, M. G.; Walkinshaw, M. D. X-ray structure of a decameric cyclophilin-cyclosporin crystal complex. *Nature* **1993**, *361*, 91−94.
(30) Theriault, Y.; Logan, T. M.; Meadows, R.; Yu, L.; Olejniczak, E. T. Holzman, T. F.; Simmer, R. L.; Fesik, S. W. Solution structure of the cyclosporin A/cyclophilin complex by NMR. *Nature* **1993**, *361*, 88−91.
(31) Zhao, Y.; Ke, H. Crystal structure implies that cyclophilin predominantly catalyzes the trans to cis isomerization. *Biochemistry* **1996**, *35*, 7356−7361.
(32) Li, Q.; Moutiez, M.; Charbonnier, J. B.; Vaudry, K.; Menez, A. Quemeneur, E.; Dugave, C. Design of a Gag pentapeptide analogue that binds human cyclophilin A more efficiently than the entire capsid protein: new insights for the development of novel anti-HIV-1 drugs. *J. Med. Chem.* **2000**, *43*, 1770−1779.
(33) Demange, L.; Moutiez, M.; Vaudry, K.; Dugave, C. Interaction of human cyclophilin hCyp-18 with short peptides suggests the existence of two functionally independent subsites. *FEBS Lett.* **2001**, *505*, 191−195.
(34) Berman, H. M.; Westbrook, J.; Feng, Z.; Gilliland, G.; Bhat, T. N. Weissig, H.; Shindyalov, I. N.; Bourne, P. E. The Protein Data Bank. *Nucleic Acids Res.* **2000**, *28*, 235−242.
(35) Gasteiger, J.; Marsili, M. Iterative partial equalization of orbital electronegativity: a rapid access to atomic charges. *Tetrahedron* **1980**, *36*, 3219−3228.
(36) Morris, G. M.; Goodsell, D. S.; Halliday, R. S.; Huey, R.; Hart, W. E. Belew, R. K.; Olson, A. J. Automated Docking Using a Lamarckian Genetic Algorithm and Empirical Binding Free Energy Function. *J. Comput. Chem.* **1998**, *19*, 1639−1662.
(37) Weiner, S. J.; Kollman, P. A.; Nguyen, D. T.; Case, D. A. An All Atom Force Field for Simulations of Proteins and Nucleic Acids. *J. Comput. Chem.* **1986**, *7*, 230−252.
(38) Mehler, E. L.; Solmajer, T. Electrostatic effects in proteins: comparison of dielectric and charge models. *Protein Eng.* **1991**, *4*, 903−910.
(39) Sybyl, version 6.8; Tripos Associates: St. Louis, MO, 2000.
(40) Cramer, M.; Cramer, R. D., III; Jones, D. M. Comparative molecular field analysis. 1. Effect of shape on binding of steroids to carrier proteins. *J. Am. Chem. Soc.* **1988**, *110*, 5959−5967.
(41) Klebe, G.; Abraham, U.; Mietzner, T. Molecular similarity indices in a comparative analysis(CoMSIA) of drug molecules to correlate and predict their biological activity. *J. Med. Chem.* **1994**, *37*, 4130−4146.
(42) Yoo, S.; Myszka, D. G.; Yeh, C.; McMurray, M.; Hill, C. P. Sundquist, W. I. Molecular recognition in the HIV-1 capsid/cyclophilin A complex. *J. Mol. Biol.* **1997**, *269*, 780−795.
(43) Wallace, A. C.; Laskowski, R. A.; Thornton, J. M. LIGPLOT: a program to generate schematic diagrams of protein−ligand interactions. *Protein Eng.* **1995**, *8*, 127−134.
(44) Ghose, A. K.; Viswanadhan, V. N.; Wendoloski, J. J. A knowledge-based approach in designing combinatorial or medicinal chemistry libraries for drug discovery. 1. A qualitative and quantitative characterization of known drug databases. *J. Comb. Chem.* **1999**, *1*, 55−68.
(45) Konno, M.; Ito, M.; Hayano, T.; Takahashi, N. The substrate-binding site in *Escherichia coli* cyclophilin A preferably recognizes a cis-proline isomer or a highly distorted form of the trans isomer. *J. Mol. Biol.* **1996**, *256*, 897−908.

JM020082X